2706 © 1982 The Chemical Society of Japan Bull. Chem. Soc. Jpn., 55, 2706—2714 (1982) [Vol. 55, No. 9

The Oxidation of Carbon Monoxide on Pt/Al_2O_3 Containing a Metal Oxide

Yukio Kosaki,* Akira Miyamoto, and Yuichi Murakami
Department of Synthetic Chemistry, Faculty of Engineering, Nagoya University, Furo-cho, Chikusa-ku, Nagoya 464

(Received November 25, 1981)

By using a three-way catalyst containing a metal oxide, CO is removed as CO_2 even in the "rich" region of the air/fuel ratio. In order to elucidate the mechanism of this action of the added metal oxide, the reaction of CO with O_2 on a Pt–V_2O_5/Al_2O_3 catalyst was investigated using a rectangular pulse-reaction apparatus. In the CO–O_2 reaction on a Pt/Al_2O_3 catalyst, a significant amount of unreacted CO was exhausted in the "rich" region of the reactants. Furthermore, the conversion of CO decreased markedly with an increase in the CO/O_2 ratio in the reactants. In the CO–O_2 reaction on the Pt–V_2O_5/Al_2O_3 catalyst, on the other hand, the conversion of CO was high and did not decrease markedly with an increase in the CO/O_2 ratio in the "rich" region. As for the reaction on the Pt–V_2O_5/Al_2O_3 at 558 K and above, the CO was completely removed as CO_2 at any of the CO/O_2 ratios examined. These effects of the added V_2O_5 were found to be due to: (i) the reaction of CO with an oxygen of V_2O_5 in the Pt–V_2O_5/Al_2O_3 catalyst and (ii) the enhanced oxidation of CO with a gaseous O_2 on the Pt/Al_2O_3 catalyst upon the addition of V_2O_5. On the basis of the kinetics of the oxidation of CO with the oxygen of V_2O_5 in the Pt–V_2O_5/Al_2O_3 and Pt black–V_2O_5 mixtures, its mechanism was proposed to be as follows; the oxygen of V_2O_5 at the Pt–V_2O_5 interface is activated by contact with Pt (this activated oxygen is denoted by [Pt···O···V]). The oxidation of CO with the oxygen of the Pt–V_2O_5/Al_2O_3 and Pt black–V_2O_5 mixtures proceeds according to the following two steps. Step I is the reaction of a gaseous CO with the active oxygen at the Pt–V_2O_5 interface, [Pt···O···V], to form CO_2 and a reduced site, [Pt V]. Step II is the oxidation of the reduced site with the bulk oxygen in V_2O_5 to reproduce [Pt···O···V]. The enhanced oxidation of CO with a gaseous O_2 caused by the addition of V_2O_5 to Pt/Al_2O_3 was found also to be understandable in terms of the active site, [Pt···O···V], where the reduced site, [Pt V], is oxidized by the gaseous O_2 to reproduce [Pt···O···V] instead of the bulk oxygen in V_2O_5.

The three-way catalyst system is used for the simultaneous removal of nitrogen monoxide, carbon monoxide, and hydrocarbons in automotive exhaust emissions.[1–5] Furthermore, attention has been focused on finding a three-way catalyst containing a metal oxide in order to deal with the fluctuation in the air/fuel ratio and broaden the "window" width.[6,7] It has been found, for the reaction of synthetic exhaust gas, that the conversion of CO in the "rich" region is much increased by the addition of a metal oxide to a three-way catalyst.[7,8] Although the mechanisms of the CO–O_2 reaction on precious metal[9–17] and metal oxide[18–21] catalysts have been the subject of many investigations, the mechanism of the action of a metal oxide added to a three-way catalyst in the CO–O_2 reaction has scarcely been investigated. The purpose of this study, then, was to establish the mechanism of the action of V_2O_5 in the CO–O_2 reaction on a Pt–V_2O_5/Al_2O_3 catalyst, particularly the mechanism of the reaction in the "rich" region. The CO–O_2 reaction was investigated, since this reaction is one of the most important reactions involved in the real three-way catalyst system.[22,23] The reason why V_2O_5 was chosen as the metal oxide has already been described in a previous paper,[24] where a mechanism of the action of the V_2O_5 in the NO–H_2 reaction on the Pt–V_2O_5/Al_2O_3 catalyst has been proposed. It should also be noted that a rectangular pulse-reaction technique was employed in this study in order to investigate the kinetics of the reaction more precisely than the conventional pulse-reaction technique makes possible. The pulse-reaction technique is considered to be useful for the investigation of the effect of the addition of a metal oxide to a three-way catalyst.[24] Furthermore, it seemed interesting to compare the synergistic effect between Pt and V_2O_5 in the CO–O_2 reaction with that in the NO–H_2 reaction.

Experimental

Catalysts. A Pt/Al_2O_3 catalyst (the Pt loading was 0.5 wt%) was purchased from Nippon Engelhard, Ltd. The Pt–V_2O_5/Al_2O_3 (the Pt loading was 0.5 wt%, and, unless otherwise specified, the content of V_2O_5 in the catalyst was 9 wt%, although a catalyst with a 36 wt% V_2O_5 loading was also used), Pt/Al_2O_3–V_2O_5(M) (the ratio of Pt/Al_2O_3 to V_2O_5 was 1/1 in weight), and Pt black–V_2O_5(P) (the ratio of Pt black to V_2O_5 was 1/1 in weight) were the same as the catalysts used in the previous study.[24] The Pt black and Pd black were purchased from Mitsuwa's Pure Chemicals Co. The Rh black was prepared using the method employed by Feulgen.[25] The precious metal black–metal oxides(M), that is, Pt black–V_2O_5(M), Pd black–V_2O_5(M), Rh black–V_2O_5(M), Pt black–MoO_3(M), Pt black–WO_3(M), and Pt black–Cr_2O_3(M), were prepared by mixing powders of the precious metal black and the metal oxide in a mortar for 20 min without water.

Characterizations of the catalysts were made by means of X-ray diffraction on a GFD-35, by scanning-electron microscope on JSM-T 20, by ESR on JES ME 1X, by IR on JASCO EDR-31,[26] and by UV on UVIDEC-505. The number of surface Pt atoms on the Pt/Al_2O_3 catalyst was determined using a conventional hydrogen adsorption apparatus.

Reagents. Commercial CO (99.9% purity) and O_2 (99.9% purity) were used without further purification. The helium used as a carrier gas was purified with a titanium metal sponge heated at 1073 K and a Molecular Sieve column at room temperature.

Apparatus and Procedure. Experiments were conducted using the rectangular pulse-reaction apparatus shown in Fig. 1. Reactants of given compositions were prepared and stor-

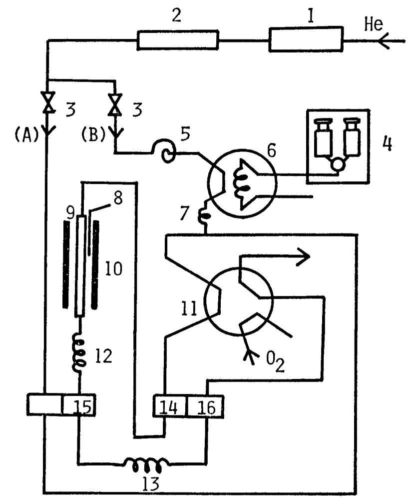

Fig. 1. A rectangular pulse reaction apparatus.
1: Titanium metal sponge deoxygenizer, 2: Molecular Sieve, 3: pressure regulator; 4: 200 ml syringes, 5: cupper tube, 6: 6-way valve for sampling, 7: stainless steel capillary, 8: thermocouple, 9: reactor, 10: electric furnace, 11: 6-way valve for O_2 treatment, 12: Porapak Q column, 13: Molecular Sieve type 13X column, 14: TCD for detecting an inlet shape of a mixture of CO and O_2, 15: TCD for detecting the shape of outlet CO_2, 16: TCD for measuring the amount of the outlet CO or O_2, (A), main stream of the carrier gas; (B), stream of the pusher gas.

ed in two syringes (4), and the sampling loop of a 6-way valve (6) was filled by means of them. The 6-way valve was turned so that the reactant gas in the sampling loop could be pushed out through a stainless steel capillary (7) to the main stream of the carrier gas (Stream A) and then carried to the reactor (9). Before all of the reactant gas in the sampling loop had been pushed out from the sampling loop, the 6-way valve (6) was returned. In such a way, the rectangular pulse could be obtained. The concentration was varied by changing the composition of the sample gas and the flow rates of the carrier gas and pusher gas. The pulse width was varied by changing the time interval between turning and returning the 6-way valve (6). The shape of the input pulse was recorded by means of a thermal conductivity detector, TCD, (14). The shape of the CO_2 produced by the oxidation of CO was observed by means of TCD (15). The carrier-gas flow rate and the length of the Porapak Q column (12) were regulated so that the shape of the CO_2 detected by means of TCD (15) gave the best rectangular pulse. The conversions of the unreacted CO and O_2 were also measured by using TCD (16). Unless otherwise specified, experiments were carried out under the following conditions. The carrier gas flow rate was 31 cm^3-STP/min, and the length of the Porapak Q column was 2 m. The pulse width was 1.5 min, and the total amount of a single pulse was 5 cm^3-STP. The concentrations of CO were 0.26—10.3%. The reaction temperatures were 341—773 K.

Results

Shapes of the Inlet Reactants and Outlet CO_2. Figure 2(a) shows an example of the Shape of the inlet mixture of CO and O_2. It was almost rectangular except for a small tailing at the front and tail of the pulse. This indicates a constant concentration of individual reactants in a pulse, a behavior significantly different from that of a conventional pulse technique. Figure 2(b) shows the shape of the CO_2 pulse detected by TCD (15) when CO_2 was pulsed instead of a mixture of CO and O_2. The concentration of CO_2 detected was independent of the time except for that at the front and tail of the pulse. This means that the shape of CO_2 is not deformed by the Porapak Q column [(12) in Fig. 1] except for the front and tail of the pulse. This also means that the rate of CO_2 formation, R_{CO_2}, can be measured from the shape of the outlet CO_2; for example, a constant concentration of CO_2 indicates a constant R_{CO_2}, because the flow rate of the carrier gas was constant. It was found that the dispersion at the front and tail of the outlet CO_2 is mainly caused when the CO_2 pulse passes through the Porapak Q column.

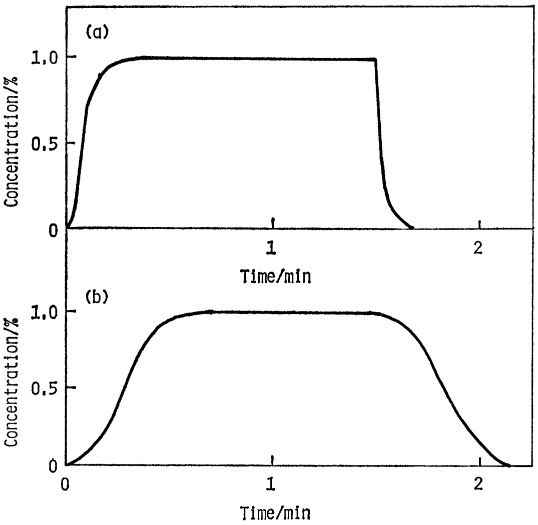

Fig. 2. Shapes of the inlet reactants and outlet CO_2.
(a): Concentration profile for the inlet mixture of CO and O_2 detected by TCD (14) (inlet concentration of the mixture=1.0%), (b): concentration profile for the CO_2 detected by TCD (15) when CO_2 is introduced (inlet concentration of CO_2=1.0%). Carrier gas flow rate=31 cm^3/min. Pulse width=90 s (total amount of a single pulse=5 cm^3-STP).

The CO–O_2 Reaction on the Pt/Al_2O_3 and Pt–V_2O_5/Al_2O_3 Catalysts. Figures 3 and 4 show the results of the CO–O_2 reaction on the Pt/Al_2O_3 and Pt–V_2O_5/Al_2O_3 catalysts at various inlet CO/O_2 ratios. The unsupported V_2O_5 or V_2O_5/Al_2O_3 was inactive for the CO–O_2 reaction under the experimental conditions used in this study. As is shown in Fig. 3, the conversion of CO (X_{CO}) for the Pt–V_2O_5/Al_2O_3 catalyst was larger than that of X_{CO} for the Pt/Al_2O_3 catalyst under any conditions shown in this figure. Although the X_{CO} for the Pt/Al_2O_3 catalyst decreased abruptly in the "rich" region (*i.e.*, $CO/O_2>2$) with an increase in the CO/O_2 ratio, the X_{CO} for the Pt–V_2O_5/Al_2O_3 catalyst did not decrease markedly with an increase in the CO/O_2 ratio. Even in the absence of gaseous O_2 ($CO/O_2=\infty$), the X_{CO} for the Pt–V_2O_5/Al_2O_3 catalyst was quite high, indicating a significant contribu-

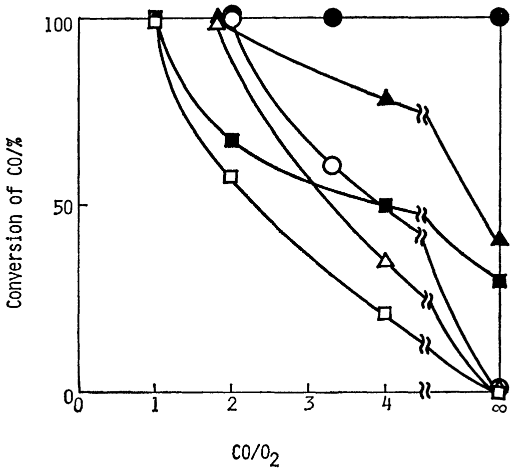

Fig. 3. Effect of the CO/O_2 ratio on the conversion of CO (X_{CO}) in the $CO-O_2$ reaction on the Pt/Al_2O_3 and $Pt-V_2O_5/Al_2O_3$ catalysts at various temperatures. ○,●: 558 K, △,▲: 448 K, □,■: 423 K (open symbols, Pt/Al_2O_3; closed symbols, $Pt-V_2O_5/Al_2O_3$). Catalyst weight; Pt/Al_2O_3=200 mg, $Pt-V_2O_5/Al_2O_3$=218 mg (Pt weight in catalysts=1 mg). Concentration of CO=1.0%.

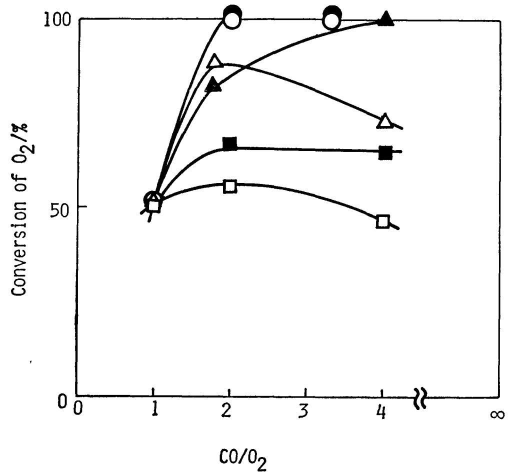

Fig. 4. Effect of the CO/O_2 ratio on the conversion of O_2 (X_{O_2}) in the $CO-O_2$ reaction on the Pt/Al_2O_3 and $Pt-V_2O_5/Al_2O_3$ catalysts at various temperatures. ○,●: 558 K, △,▲: 448 K, □,■: 423 K (open symbols, Pt/Al_2O_3; closed symbols, $Pt-V_2O_5/Al_2O_3$). Catalyst weight; Pt/Al_2O_3=200 mg, $Pt-V_2O_5/Al_2O_3$=218 mg (Pt weight in catalysts=1 mg). Concentration of CO=1.0%.

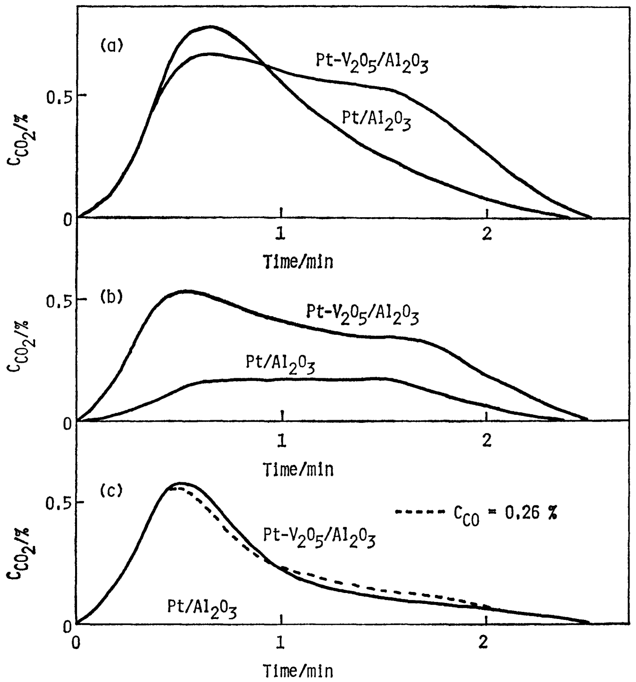

Fig. 5. Shapes of the outlet CO_2 in the $CO-O_2$ reaction on the Pt/Al_2O_3 and $Pt-V_2O_5/Al_2O_3$ catalysts at 423 K.
(a): CO/O_2=2.0, (b): CO/O_2=4.0, (c): CO/O_2=∞ (concentration of CO=1.0%). Catalyst weight; Pt/Al_2O_3=200 mg, $Pt-V_2O_5/Al_2O_3$=218 mg (Pt weight in catalysts=1 mg).

tion of the oxygen of V_2O_5 to the oxidation of CO. For the reaction on this catalyst at temperatures above 558 K, CO was completely oxidized (*i.e.*, X_{CO}=100%), irrespective of the inlet CO/O_2 ratio. These data clearly indicate that the added V_2O_5 plays an important role in the oxidation of CO on the $Pt-V_2O_5/Al_2O_3$ catalyst. As is shown in Fig. 4, the conversion of O_2 (X_{O_2}) in the "rich" region for the $Pt-V_2O_5/Al_2O_3$ catalyst was higher than X_{O_2} for the Pt/Al_2O_3 catalyst. This indicates that the oxidation of CO with a gaseous O_2 on Pt/Al_2O_3 is also promoted by the addition of V_2O_5 to Pt/Al_2O_3.

Concentration Profiles of the CO_2 Produced by the Oxidation of CO on the Pt/Al_2O_3 and $Pt-V_2O_5/Al_2O_3$ Catalysts. Figure 5 shows the concentration profiles of the CO_2 produced by the oxidation of CO under various conditions. Since the flow rate of the carrier gas was constant, the measured concentration of CO_2 at a given time is proportional to R_{CO_2} at this same time. As is shown in Fig. 5(a), the R_{CO_2} on Pt/Al_2O_3 at the stoichiometric point (*i.e.* CO/O_2=2) decreased markedly with the time after its maximum. On the other hand, the R_{CO_2} on the $Pt-V_2O_5/Al_2O_3$ catalyst decreased only slightly with the time; in fact, it was almost independent of the time. As for the reaction in the "rich" region (*i.e.*, CO/O_2=4)[Fig. 5(b)], the R_{CO_2} on the Pt/Al_2O_3 catalyst was significantly slower than the R_{CO_2} on the $Pt-V_2O_5/Al_2O_3$ catalyst. It is also noted that the R_{CO_2} for the $Pt-V_2O_5/Al_2O_3$ catalyst decreases slightly with an increase in the time. As for the reaction in the absence of gaseous O_2(*i.e.*, CO/O_2=∞)[Fig. 5(c)], the R_{CO_2} on the $Pt-V_2O_5/Al_2O_3$ catalyst decreased markedly with the time; on the other hand, no CO_2 was produced on the Pt/Al_2O_3 catalyst, irrespective of the time. It can also be noted in Fig. 5(c) that the R_{CO_2} for the reaction on $Pt-V_2O_5/Al_2O_3$ in the absence of O_2 is independent of the concentration of CO.[27] This can also be seen in the relationship between the yield of CO_2(Y_{CO_2}) and the concentration of CO(C_{CO}; 1%=2.24 μmol/cm^3 under the experimental conditions in this study) shown in Fig. 6; Y_{CO_2} was independent of C_{CO} at both 341 and 423 K.[27]

Kinetics of the Oxidation of CO with the Oxygen of Metal

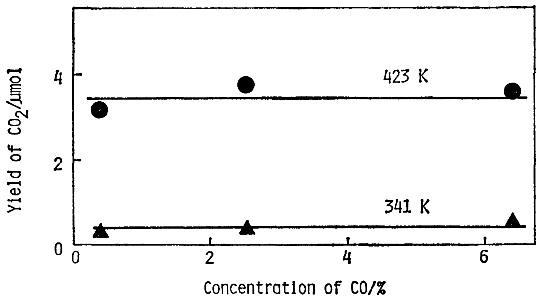

Fig. 6. Effect of the concentration of CO on the reaction of CO with the $Pt-V_2O_5/Al_2O_3$ catalyst at various temperatures.
●: 423 K, ▲: 341 K. Catalyst weight=218 mg.

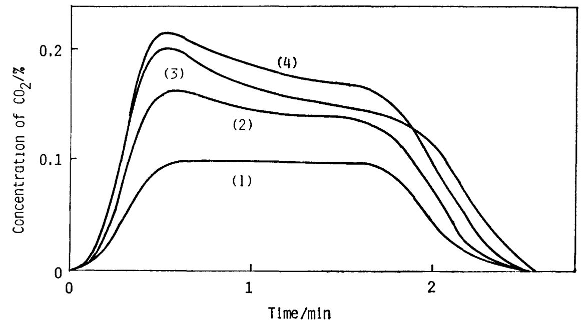

Fig. 7. Shapes of the outlet CO_2 in the reaction of CO with the 5 wt% Pt black–V_2O_5(M) catalyst at 504 K.
(1): Concentration of CO=1.0%, (2): concentration of CO=2.0%, (3): concentration of CO=5.0%, (4): concentration of CO=6.5%. Catalyst weight=40 mg.

Oxides. Since the unsupported V_2O_5 or V_2O_5/Al_2O_3 was inactive for the reaction with CO, the formation of CO_2 observed for the $Pt-V_2O_5/Al_2O_3$ [Fig. 5(c)] is due to the oxidation of CO with the oxygen of V_2O_5 promoted by Pt. However, as is shown in Fig. 5(c), the R_{CO_2} for the $Pt-V_2O_5/Al_2O_3$ catalyst changes greatly with the time, which makes it difficult to investigate the mechanism of the synergistic effect between Pt and V_2O_5. This is the reason why various mixtures of precious metal and metal oxide were used in this study as catalysts for investigating the mechanism of the reaction of CO with the oxygen of metal oxides promoted by precious metals.[28] The $Pt/Al_2O_3-V_2O_5$(M) or Pt black–V_2O_5 (P) did not oxidize CO to CO_2 under the present experimental conditions. Pt black–V_2O_5(M) was active for the oxidation of CO, and, as is shown in Fig. 7, R_{CO_2} did not change significantly with the time. Similarly, the R_{CO_2} on Pd black–V_2O_5(M), Rh black–V_2O_5(M), and Pt black–MoO_3(M) was almost independent of the time. The Pt black–WO_3(M) or Pt black–Cr_2O_3(M) was inactive for the reaction. Therefore, the Pt black–V_2O_5(M), Pd black–V_2O_5(M), Rh black–V_2O_5(M), and Pt black–MoO_3(M) are considered to be catalysts which can be used for detailed investigations of the mechanism of the synergistic effect between a precious metal and a metal oxide on the oxidation of CO with the oxygen of the metal oxide.

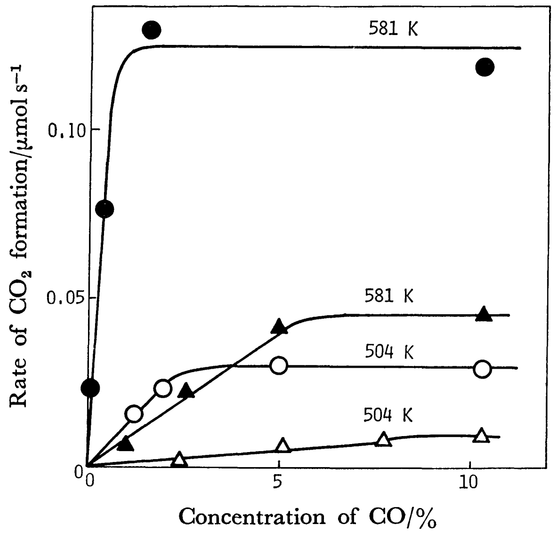

Fig. 8. Effect of the concentration of CO on the reaction of CO with 1 and 5 wt% Pt black–V_2O_5(M) catalysts at various temperatures.
●,▲: 581 K, ○,△: 504 K [circle symbols, 5 wt% Pt black–V_2O_5(M); triangle symbols, 1 wt% Pt black–V_2O_5(M)]. Catalyst weight=40 mg.

Figure 8 shows some of the findings regarding R_{CO_2} for the reaction of CO with Pt black–V_2O_5(M) at various C_{CO} values. Here, R_{CO_2} is calculated from the average value of R_{CO_2} at the plateau of the concentration profile shown in Fig. 7. As is shown in Fig. 8, R_{CO_2} was of the first order with respect to C_{CO} when C_{CO} was low(this region will hereafter be referred to as R1). When C_{CO} was high, R_{CO_2} was of the zeroth order with respect to C_{CO}(this region will hereafter be referred as R0). The boundary between R1 and R0 for 1 wt% Pt black–V_2O_5(M) was located at C_{CO}, higher than that for 5 wt% Pt black–V_2O_5(M). It may also be noted in Fig. 8 that the boundary between R1 and R0 moves to a lower C_{CO} with an increase in the reaction temperature. From the observed R_{CO_2} values at various C_{CO} levels, the first-order and zeroth-order rate constants were determined. These rate constants, measured at various temperatures, satisfied the Arrhenius equations, and the activation energies(E_1 and E_0) and pre-exponential factors(A_1 and A_0) were determined to be as is shown in Table 1. Here, A_1 and A_0 are normalized to have a unit weight of the precious metal. The Arrhenius parameters were also determined for the Pd black–V_2O_5(M), Rh black–V_2O_5(M), and Pt black–MoO_3 (M) catalysts; these are also shown in Table 1. The E_1 for 1 wt%Pt black–V_2O_5(M) was almost the same as the E_1 for 5 wt% Pt black–V_2O_5(M); on the other hand, both values are larger than the E_1 for Pd black–V_2O_5(M) or Rh black–V_2O_5(M). The E_0 for 1 and 5 wt% Pt black–V_2O_5(M), Pd black–V_2O_5(M), and Rh black–V_2O_5(M) was almost constant and independent of the kind of catalyst. However, the E_0 for Pt black–MoO_3(M) was larger than the E_0 for the former catalysts. The A_1 or A_0 did not change markedly with the kind of catalyst; that is, the A_1 and A_0 changed at the maximum by factors of only

Table 1. The activation energies and pre-exponential factors in the reaction of CO with the cataly

Catalyst	R1		R0	
	$\frac{E_1}{\text{kcal mol}^{-1}}$	$\frac{A_1}{\text{cm}^3\ \text{s}^{-1}\ \text{g-metal}^{-1}}$	$\frac{E_0}{\text{kcal mol}^{-1}}$	$\frac{A_0}{\text{mol s}^{-1}\ \text{g-metal}^{-1}}$
1 wt% Pt black-V_2O_5(M)	17.3	1.4×10^8	11.5	2.6
5 wt% Pt black-V_2O_5(M)	16.4	1.7×10^8	11.8	2.2
1 wt% Pd black-V_2O_5(M)	13.6	0.2×10^8	12.2	12
1 wt% Rh black-V_2O_5(M)	13.7	0.6×10^8	12.6	7.1
1 wt% Pt black-MoO_3(M)	—[a]	—[a]	15.0	4.9
Pt-V_2O_5/Al_2O_3	—[a]	—[a]	10.3[b] (10.4)[c]	40[b] (116)[c]

a) The R1 region did not appear under the experimental conditions used in this study. b) Values calculated from the average R_{CO_2}. c) Values calculated from the maximum R_{CO_2}.

7 and 5 respectively. The A_0 and E_0 for Pt–V_2O_5/Al_2O_3 were similarly determined, though these values are considered not to be correct for the reasons presented above. The E_0 for Pt–V_2O_5/Al_2O_3 was slightly lower than the E_0 for Pt black–V_2O_5(M), while the A_0 for Pt–V_2O_5/Al_2O_3 was about 20 times larger than the A_0 for Pt black–V_2O_5(M).

Characterizations of the Pt–V_2O_5/Al_2O_3 and Pt Black–V_2O_5(M) Catalysts. The number of surface Pt atoms on the Pt/Al_2O_3 catalyst was determined, by using the H_2 adsorption technique, to be 5.0 μmol/g-cat, which leads to an average Pt diameter of 30 Å. The X-ray diffraction pattern of Pt black–V_2O_5(M) indicated that it is a mixture of Pt metal and V_2O_5 crystallines; therefore, no other compound was detected. On the basis of the SEM measurements of Pt black–V_2O_5(M), the average diameters of Pt and V_2O_5 in the catalyst were determined to be 5000 and 2000 Å respectively. ESR, IR, and UV measurements of Pt–V_2O_5/Al_2O_3 and Pt black–V_2O_5(M) indicated that the vanadium oxides in these catalysts are mainly in the highest oxidation state, *i.e.*, V^{5+}. The structure of V_2O_5 in V_2O_5/Al_2O_3 catalysts with various contents of V_2O_5 has been determined by using the NO–NH_3 rectangular pulse technique, coupled with the IR, ESR, and UV techniques.[29]

Discussion

Removal of CO in the "Rich" Region Using the Pt–V_2O_5/Al_2O_3 Catalyst. As is shown in Fig. 3, CO is almost completely removed in the "lean" region of the reactants (*i.e.*, $CO/O_2<2$) by using the Pt/Al_2O_3 catalyst. However, the X_{CO} in the CO–O_2 reaction in the "rich" region (*i.e.*, $CO/O_2>2$) decreases markedly with an increase in the CO/O_2 ratio. This means that a considerable amount of unreacted CO is exhausted in the "rich" region. This behavior in the CO–O_2 reaction on the Pt/Al_2O_3 catalyst is similar to that in the reactions of synthetic exhaust gas in three-way catalysts without metal oxides.[22,23] The X_{CO} in the reaction on the Pt–V_2O_5/Al_2O_3 catalyst is high even in the "rich" region. As for the reaction at temperatures above 558 K, X_{CO} is 100% at any CO/O_2 ratio, indicating a complete removal of CO. This behavior in the CO–O_2 reaction on the Pt–V_2O_5/Al_2O_3 catalyst is similar to that in the reactions of synthetic exhaust gas on three-way catalysts containing metal oxides.[7,8]

The Amounts of Gaseous O_2 and Oxygen of V_2O_5 Consumed for the Oxidation of CO on the Pt–V_2O_5/Al_2O_3 Catalyst. In addition to a gaseous O_2, the oxygen of V_2O_5 participates in the oxidation of CO on the Pt–V_2O_5/Al_2O_3 catalyst (Fig. 3). Also, as is shown in Fig. 4, the oxidation of CO with a gaseous O_2 on the Pt/Al_2O_3 catalyst is promoted by the addition of V_2O_5 to the catalyst. It is, therefore, necessary to calculate the amounts of gaseous O_2 [Q_G(Pt) and Q_G(Pt–V)] and the oxygen of V_2O_5 [Q_V(pt) and Q_V(Pt–V)] consumed for the oxidation of CO on the Pt/Al_2O_3 and Pt–V_2O_5/Al_2O_3 catalysts before discussing in detail the mechanism of the action of the added V_2O_5. In the pulse experiment, material balances with respect to the oxygen atoms lead to the following equations:

$$Q_G(\text{Pt}) = 2Q_{O_2}^{\circ}\cdot X_{O_2}(\text{Pt}), \tag{1}$$

$$Q_V(\text{Pt}) = Q_{CO_2}(\text{Pt}) - Q_G(\text{Pt}), \tag{2}$$

$$Q_G(\text{Pt-V}) = 2Q_{O_2}^{\circ}\cdot X_{O_2}(\text{Pt-V}), \tag{3}$$

$$Q_V(\text{Pt-V}) = Q_{CO_2}(\text{Pt-V}) - Q_G(\text{Pt-V}), \tag{4}$$

where Q_G is the number of oxygen atoms in O_2 consumed for the oxidation of CO; Q_V is the number of the oxygen of V_2O_5 consumed for the oxidation of CO; $Q_{O_2}^{\circ}$ is the number of gaseous O_2 injected as a reactant of the pulse experiment; X_{O_2} is the conversion of O_2; Q_{CO_2} is the number of CO_2 molecules produced; and (Pt) and (Pt–V) refer to the Pt/Al_2O_3 and Pt–V_2O_5/Al_2O_3 catalysts respectively. On the basis of the experimental results for the Pt/Al_2O_3 catalyst shown in Figs. 3 and 4, Eq. 2′ is obtained for Q_V(Pt):

$$Q_V(\text{Pt}) = 0. \tag{2′}$$

This relationship is reasonable, since the Pt/Al_2O_3 catalyst does not contain V_2O_5. From Eqs. 1 and 3, the increase in Q_G caused by the addition of V_2O_5 to Pt/Al_2O_3(ΔQ_G) is given by Eq. 5:

$$\Delta Q_G = Q_G(\text{Pt-V}) - Q_G(\text{Pt}). \tag{5}$$

Similarly, from Eqs. 2′ and 4 the increase in Q_V(ΔQ_V)

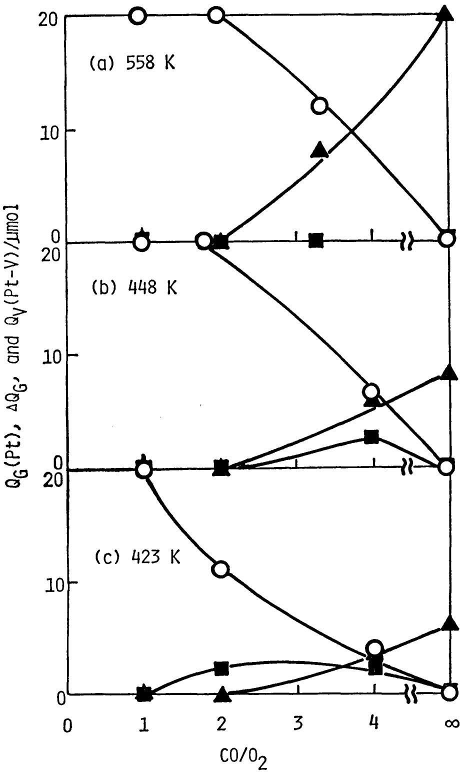

Fig. 9. Relationship between the CO/O_2 ratio and Q_G(Pt), ΔQ_G, and Q_V(Pt–V) in the CO–O_2 reaction on the Pt–V_2O_5/Al_2O_3 catalyst.
○: Q_G(Pt), ■: ΔQ_G, ▲: Q_V(Pt–V). Concentration of CO=1.0%. Catalyst weight=218 mg.

is given by Eq. 6:

$$\Delta Q_V = Q_V(\text{Pt–V}). \tag{6}$$

Figure 9 shows the results for Q_G(Pt), ΔQ_G, and Q_V(Pt–V), which were calculated from the experimental results shown in Figs. 3 and 4. As is shown in Fig. 9, Q_G(Pt) mainly contributes to the CO–O_2 reaction on the Pt–V_2O_5/Al_2O_3 catalyst in the "lean" region (CO/O_2<2), and the synergistic effect between Pt and V_2O_5, *i.e.*, ΔQ_G or Q_V(Pt–V), is not important. As the CO/O_2 ratio increases in the "rich" region (CO/O_2>2), Q_G(Pt) decreases, but Q_V(Pt–V) and ΔQ_G become significant. In particular, Q_V(Pt–V) mainly contributes to the reaction in the "rich" region. It should also be noted that ΔQ_G plays an important role in the reaction in the "rich" region at temperatures as low as 423 K.

Structures of Pt–V_2O_5/Al_2O_3 and Pt Black–V_2O_5(M). On the basis of the above-mentioned characterizations of Pt–V_2O_5/Al_2O_3 and Pt black–V_2O_5(M), the structures of these catalysts shown in Fig. 10 can be proposed. The average diameter of Pt particles on Pt–V_2O_5/Al_2O_3 is about 30 Å, which has been determined by the H_2 adsorption measurement. In the V_2O_5/Al_2O_3 catalyst(V_2O_5 loading is 9 wt%), 1—2 layers of V_2O_5 lamellae cover a small percentage of the Al_2O_3 surface.[29] Since the content of Pt is very low (0.5 wt%), the V_2O_5 in the Pt–V_2O_5/Al_2O_3 catalyst is considered to be almost the same as the V_2O_5 in the V_2O_5/Al_2O_3 catalyst. The coverage of V_2O_5 and the particle size of Pt thus determined lead to the structure of V_2O_5 and Pt on Al_2O_3, indicating that Pt particles are partly in contact with V_2O_5 and are partly separated from V_2O_5. The vanadium oxides in the Pt–V_2O_5/Al_2O_3 catalyst are mainly in the highest oxidation state, *i.e.*, V^{5+}, judging from the ESR and UV measurements of Pt–V_2O_5/Al_2O_3. On the basis of the SEM and XRD investigations of Pt black–V_2O_5(M), the structure shown in Fig. 10(b) can be proposed; Pt black–V_2O_5(M) is a mixture of Pt black(about 5000 Å in diameter) and V_2O_5 particles(about 2000 Å in diameter). The V_2O_5 in Pt black–V_2O_5(M) is composed of about 500 layers of V_2O_5 lamellae.

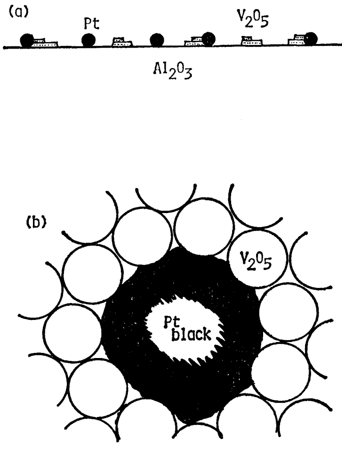

Fig. 10. Structures of Pt–V_2O_5 mixed catalysts.
(a): Pt–V_2O_5/Al_2O_3; the average diameter of Pt particles is about 30 Å, 1—2 layers of V_2O_5 lamella cover a few percentage of the Al_2O_3 surface, (b): Pt black–V_2O_5(M); a Pt black particle (about 5000 Å in diameter) is surrounded by many V_2O_5 particles [about 2000 Å in diameter (about 500 layers of V_2O_5 lamella)].

Mechanism of the Oxidation of CO with the Oxygen of V_2O_5 in Pt Black–V_2O_5(M). From the experimental results shown in Table 1 and in Figs. 7 and 8, the mechanism of the oxidation of CO with the oxygen of V_2O_5 in Pt black–V_2O_5(M) shown in Fig. 11(a) can be proposed. According to this mechanism, the oxygen of V_2O_5 at the Pt–V_2O_5 interface is activated by contact with Pt; this is a new type of active site and will hereafter be denoted by [Pt···O···V]. Also, the oxidation of CO with the oxygen of Pt black–V_2O_5(M) proceeds according to the following two steps. Step I is the reaction of a gaseous CO with the active oxygen at the Pt–V_2O_5 interface, [Pt···O···V], to form CO_2 and a reduced site, [Pt V]. Step II is the oxidation of the reduced site, [Pt V], with the bulk oxygen in V_2O_5 to reproduce [Pt···O···V]. The validity of this mechanism can be proved as follows.

Kinetics: Since Step I is the reaction of a gaseous CO with the activated surface oxygen, its rate will increase with the increase in the concentration of CO. Since a gaseous CO does not participate in Step II, on the other hand, the rate of Step II will be independent of C_{CO}. Therefore, the rate of Step I relative to Step II would decrease with a decrease in C_{CO}. In other words, Step I becomes the rate-

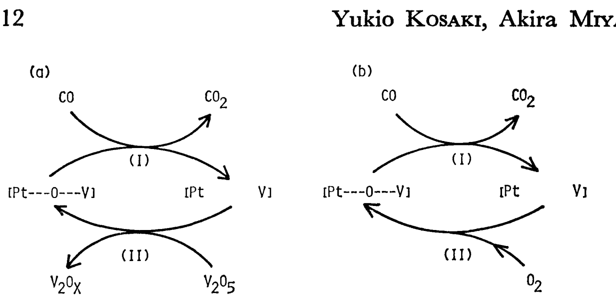

Fig. 11. Mechanism of the CO–O_2 reaction on Pt–V_2O_5 mixed catalysts.
(a): Mechanism of the oxidation of CO with the oxygen of V_2O_5 in the Pt black–V_2O_5(M) catalyst, (b): mechanism of the oxidation of CO with a gaseous O_2 caused by the synergistic effect between Pt and V_2O_5 [ΔQ_G].

determining step when C_{CO} is low. On the other hand, when C_{CO} is high, Step II becomes the rate-determining step. This is in accordance with the observed kinetics shown in Fig. 8, because the rate is of the first order with respect to C_{CO} when C_{CO} is low, while it is of the zeroth order when C_{CO} is high.

Activation Energies: Judging from the above-mentioned discussion on the kinetics of the reaction, E_1 and E_0 can be regarded as the activation energies of Steps I and II respectively. Since a precious metal plays an important role in Step I of the mechanism shown in Fig. 11(a), E_1 should vary depending on the kind of precious metal used. Step II is the migration of the bulk oxygen atom of a metal oxide to its surface, followed by the interaction of the surface oxygen atom with Pt. Since the adsorption of an atomic oxygen on the Pt surface is considered to be a non-activated process, the migration of the bulk oxygen to the surface may limit the rate of Step II. This leads to the value of E_0, which should be independent of the kind of precious metal, but which should change with the kind of metal oxide. This inference is in accordance with the experimental results shown in Table 1.

Boundary between R1 and R0: According to the mechanism shown in Fig. 11(a), the boundary between R1 and R0 is determined by the rate of Step I relative to Step II. Judging from the structure of Pt black–V_2O_5(M), the number of [Pt···O···V] sites can be expected to increase in proportion to the content of the Pt black. This leads to the increase in the rate of Step I in proportion to the content of the Pt black in the catalyst. Since the quantity of oxygen atoms consumed for the reaction in the R0 region was much larger than the amount of the surface oxygen atoms of V_2O_5,[29] the rate in the R0 region may refer to the rate of the diffusion of oxygen in the bulk of V_2O_5 particles, but not to the rate of the diffusion of the subsurface oxygen atoms to the reduced active site, [Pt V]. This means that the rate of Step II is less sensitive to the increase in the content of Pt black than the rate of Step I, suggesting that the rate of Step I relative to Step II increases with an increase in the content of the Pt black in the catalyst. The boundary between R1 and R0 for 5 wt% Pt black–V_2O_5(M) is thus considered to be located at a C_{CO} point lower than the C_{CO} for 1 wt% Pt black–V_2O_5(M). This is in accordance with the experimental results shown in Fig. 8.

The above discussion indicates that all of the experimental data shown in Table 1 and Figs. 7 and 8 can reasonably be understood in terms of the mechanism shown in Fig. 11(a). In order to establish the validity of the mechanism, however, a discussion of possible alternative mechanisms is indispensable.

AM-1: CO is activated on the Pt surface, migrates onto V_2O_5, and reacts with the oxygen of V_2O_5 to form CO_2.[30]

CO is not dissociatively, but molecularly, adsorbed on the Pt surface[31–34] under the present experimental conditions. V_2O_5 is not active for the reaction with a molecular CO; CO is scarcely oxidized by the oxygen of V_2O_5, even at a temperature as high as 773 K. These data indicate that AM-1 does not play an important role in the oxidation of CO with Pt black–V_2O_5(M).

AM-2: The oxygen of V_2O_5 migrates onto the surface of Pt and reacts with CO to form CO_2.

The reaction of CO with an adsorbed oxygen atom on Pt proceeds so rapidly that the activation energy for this process is low.[9,11,35] and every 10 collisions of CO molecules with the oxygen atom adsorbed on Pt lead to the formation of one CO_2 molecule, even at room temperature.[31] This is not consistent with the observed activation energy shown in Table 1.

AM-3: The CO adsorbed on the Pt surface reacts with the oxygen of V_2O_5 at the Pt–V_2O_5 interface; therefore, the R_{CO_2}–C_{CO} curves are determined by the coverage of CO on the Pt surface.

The amount of CO adsorbed on Pt decreases with an increase in the temperature.[31–33] If the boundary between R1 and R0 is determined by the coverage of the adsorbed CO, then it should move to a higher C_{CO} value as the temperature increases. However, this is not consistent with the experimental results shown in Fig. 8.

Mechanism of the Oxidation of CO on the Pt–V_2O_5/Al_2O_3 Catalyst. As has been mentioned above, the amount of CO_2 molecules produced by the CO–O_2 reaction on the Pt–V_2O_5/Al_2O_3 catalyst is determined by following three factors: Q_G(Pt), ΔQ_G, and Q_V(Pt–V). The mechanisms of the reactions responsible for the individual factors will be discussed below.[36]

The CO–O_2 Reaction on the Pt Surface[Q_G(Pt)]: The mechanism of the CO–O_2 reaction on the Pt surface has already been investigated extensively.[9–11,13,37] According to the mechanism, the CO adsorbed on Pt retards the CO–O_2 reaction at low temperatures.[9,10,38–41] In accordance with this mechanism, the observed rate of the CO–O_2 reaction on the Pt/Al_2O_3 catalyst decreases markedly with an increase in the CO/O_2 ratio at low temperatures, especially at 423 K (Fig. 3). The concentration profile of CO_2 produced by the CO–O_2 reaction on Pt/Al_2O_3 shows that the rate of CO_2 formation decreases significantly with the time [Fig. 5(a)]. This phenomenon may be interpreted in terms of the proposed mechanism of the CO–O_2 reaction on the Pt surface as follows; as the time increases, the coverage of CO on the Pt surface increases, which then leads to the decrease in the rate of the reaction with an increase in the time.

The Oxidation of CO with the Oxygen of V_2O_5 Promoted by Pt [Q_V(Pt–V)]: Since the electronic state of V_2O_5 supported on Al_2O_3 is almost the same as that of the unsupported V_2O_5, the mechanism shown in Fig. 11(a) can be applied to the reaction of CO with the oxygen of V_2O_5 in the Pt–V_2O_5/Al_2O_3 catalyst. Although the kinetics for Pt–V_2O_5/Al_2O_3 is different from that for Pt black–V_2O_5(M), this difference can be explained in terms of the structures of Pt–V_2O_5/Al_2O_3 and Pt black–V_2O_5(M) as follows. As is shown in Fig. 10, both Pt and V_2O_5 for Pt–V_2O_5/Al_2O_3 are much better dispersed than those for Pt black–V_2O_5(M). The number of the active sites, [Pt···O···V], for Pt–V_2O_5/Al_2O_3 is thus considered to be greater than that for Pt black–V_2O_5(M). This in turn leads to a rate of Step I for Pt–V_2O_5/Al_2O_3 which is faster than that for Pt black–V_2O_5(M). On the other hand, the amount of V_2O_5, which can supply oxygen atoms to the active site, is limited for Pt–V_2O_5/Al_2O_3, because the V_2O_5 on Al_2O_3 is highly dispersed. This is the reason the rate of CO_2 formation decreases markedly with the time for Pt–V_2O_5/Al_2O_3 [Fig. 5(c)] and why the R1 region does not appear in the R_{CO_2}–C_{CO} curves for Pt–V_2O_5/Al_2O_3 (Fig. 6). The A_0 for Pt–V_2O_5/Al_2O_3 is larger than the A_0 for Pt black–V_2O_5(M) (Table 1). This may also be due to the high dispersion of Pt and V_2O_5 on Al_2O_3 in Pt–V_2O_5/Al_2O_3. The E_0 for Pt–V_2O_5/Al_2O_3 is a little lower than the E_0 for Pt black–V_2O_5(M); this difference may be ascribable to the lack of a supply of the bulk oxygen in V_2O_5 at high temperatures for Pt–V_2O_5/Al_2O_3. Although the results for Pt–V_2O_5/Al_2O_3 can well be understood on the basis of the mechanism shown in Fig. 11(a), a discussion of a following alternative mechanism is indispensable:

AM-4: The oxygen of V_2O_5 migrates to the Pt surface through Al_2O_3 and reacts with CO on Pt.

As for Pt/Al_2O_3–V_2O_5(M), Pt is considered to be separated from V_2O_5 by Al_2O_3, and CO is not oxidized with the oxygen of this catalyst. Therefore, AM-4 is not important in the reaction on Pt–V_2O_5/Al_2O_3.

The Oxidation of CO with a Gaseous O_2 Caused by the Synergistic Effect between Pt and V_2O_5[ΔQ_G]: According to the mechanism of the reaction of CO with the oxygen of V_2O_5 in the Pt black–V_2O_5(M) and Pt–V_2O_5/Al_2O_3 catalysts shown in Fig. 11(a), [Pt V] is formed by the reaction of CO with the [Pt···O···V] site. If a gaseous O_2 is present in the system, [Pt V] can be expected to be oxidized by the gaseous O_2 to reproduce the [Pt···O···V] site, which may in turn increase the rate of the oxidation of CO with a gaseous O_2 on Pt–V_2O_5/Al_2O_3 more than that on Pt/Al_2O_3. This means that ΔQ_G can be explained in terms of the mechanism of the CO–O_2 reaction shown in Fig. 11(b). This mechanism is similar to the mechanism of the oxidation of CO with the oxygen of V_2O_5 shown in Fig. 11(a), but the reduced site, [Pt V], is reoxidized to [Pt···O···V] by a gaseous O_2, not by the bulk oxygen in V_2O_5. As is evident from the mechanism shown in Fig. 11(b), the reaction of CO with [Pt···O···V] is not retarded by the adsorbed CO, behavior which is different from the behavior in the CO–O_2 reaction on the Pt surface. This explains why ΔQ_G mainly contributes to the reaction in the "rich" region at low temperatures (Fig. 9). In the practical three-way catalyst system, the fluctuation in the air/fuel ratio takes place rapidly with a frequency of 1—10 Hz;[42,43] therefore a part of the CO adsorbed on Pt on the "rich" side may still remain on Pt even on the "lean" side. This suggests that the CO–O_2 reaction on Pt, [Q_G(Pt)], is retarded by the CO remaining on Pt under practical three-way catalyst conditions. Since the reaction of CO at the [Pt···O···V] site, [Q_V(Pt–V) and ΔQ_G], is not retarded by CO remaining on Pt, it may play an important role under certain conditions.

Synergistic Effect between Pt and V_2O_5 in the CO–O_2 Reaction as Compared with That in the NO–H_2 Reaction. The conversion of CO in the CO–O_2 reaction on the Pt/Al_2O_3 catalyst in the "rich" region has been markedly enhanced by the addition of V_2O_5 to Pt/Al_2O_3. This effect of V_2O_5 has been found to be brought about by the formation of a new type of active site, [Pt···O···V], at the Pt–V_2O_5 interface, which plays an important role in the oxidation of CO with the oxygen of V_2O_5 and the enhanced oxidation of CO with a gaseous O_2 on Pt/Al_2O_3 caused by the addition of V_2O_5 to Pt/Al_2O_3. The mechanism of the action of V_2O_5 in the oxidation of CO is much different from that in the NO–H_2 reaction found in the previous study.[24] In the NO–H_2 reaction on the Pt–V_2O_5/Al_2O_3 catalyst, the selective reduction of NO to N_2 or N_2O in the "rich" region is brought about by the "hydrogen spillover"—the dissociation of H_2 on Pt, followed by the spillover of the dissociated hydrogen from Pt to Al_2O_3 and then to V_2O_5 and the subsequent reduction of V_2O_5 with the spilled-over hydrogen. The synergistic effect between Pt and V_2O_5 in the NO–H_2 reaction can, therefore, appear even if Pt and V_2O_5 are separated from each other by Al_2O_3; this behavior is different from that in the CO–O_2 reaction. This means that the mechanism of the action of a metal oxide added to a three-way catalyst can change greatly depending on the kind of reaction. Since the real three-way catalyst system is composed of various types of reactions, the accumulation of investigations such as the present one can lead to the scientific development of a three-way catalyst with a sufficiently broad "window". In addition, the activity of the Pt/Al_2O_3 catalyst for the oxidation of CO with the gaseous O_2 enhanced by the addition of V_2O_5 suggests the possibility that the amount the precious metals used for the three-way catalyst system can be saved by the addition of a metal oxide to a three-way catalyst.

References

1) M. Shelef, *Catal. Rev.*, **11**, 1 (1975).
2) J. Wei, *Adv. Catal.*, **24**, 57 (1975).
3) T. Ono, *Shokubai*, **19**, 142 (1977).
4) E. Echigoya, *Kagaku*, **33**, 338 (1978).
5) H. Ohara, S. Kondo, and Y. Fujitani, *Paper of Society of Automotive Engineers of Japan*, **16**, 9 (1978).

6) J. E. Hunter, *SAE Paper*, 720201 (1972).

7) H. S. Gandhi, A. G. Pikin, M. Shelef, and R. G. Delosh, *SAE Paper*, 760201 (1976).

8) J. C. Schlatter and P. J. Mitchell, *Ind. Eng. Chem., Prod. Res. Dev.*, **19**, 288 (1980).

9) H. P. Bonzel and R. Ku, *Surf. Sci.*, **33**, 91 (1972).

10) H. P. Bonzel and R. Ku, *J. Vac. Sci. Technol.*, **9**, 633 (1972).

11) T. Matsushima, D. B. Almy, and J. M. White, *Surf. Sci.*, **67**, 89 (1977).

12) C. T. Campbell and J. M. White, *J. Catal.*, **54**, 289 (1978).

13) T. Matsushima, *Surf. Sci.*, **79**, 63 (1979).

14) T. Engel and G. Ertl, *Adv. Catal.*, **28**, 1 (1979).

15) K. Kunimori and T. Uchijima, *Hyomen*, **19**, 143 (1981).

16) E. Miyazaki, *Shokubai*, **22**, 301 (1980).

17) M. Kawai, T. Onishi, and K. Tamaru, *Shokubai*, **22**, 304 (1980).

18) F. S. Stone, *Adv. Catal.*, **13**, 1 (1962).

19) S. Yoshida, Y. Miyata, H. Niiyama, and E. Echigoya, *Shokubai*, **23**, 284 (1981).

20) K. Sakata, F. Ueda, M. Misono, and Y. Yoneda, *Bull. Chem. Soc. Jpn.*, **53**, 324 (1980).

21) T. Nakamura, M. Misono, T. Uchijima, and Y. Yoneda, *Nippon Kagaku Kaishi*, **1980**, 1679.

22) K. C. Taylor, "The Catalytic Chemistry of Nitrogen Oxides," ed by R. L. Klimisch and J. G. Larson, Plenum Press, New York, N. Y. (1975), p. 173.

23) J. Wei, *Adv. Catal.*, **24**, 57 (1976).

24) Y. Kosaki, A. Miyamoto, and Y. Murakami, *Bull. Chem. Soc. Jpn.*, **55**, 1719 (1982).

25) R. Feulgen, *Ber.*, **54**, 360 (1921).

26) M. Niwa, T. Hattori, M. Takahashi, and K. Shirai, *Anal. Chem.*, **51**, 46 (1979).

27) Similar phenomena were also observed in the reaction of CO with the Pt–V_2O_5(36 wt%)/Al_2O_3 catalyst.

28) The precious metal black–metal oxide(M) catalyst was used as a model catalyst of the Pt–V_2O_5/Al_2O_3 because it was difficult to prepare a Pt/V_2O_5 (impregnation) catalyst.

29) Y. Murakami, M. Inomata, A. Miyamoto, and K. Mori, *Proc. 7th Int. Congr. Catal., Tokyo*, 1980, Kodansha (Tokyo) and Elsevier (Amsterdam-Oxford-New York) (1981), p. 1344.

30) G. C. Bond, M. J. Fuller, and L. R. Molloy, *Proc. 6th Int. Congr. Catal., London*, 1976, The Chemical Society (1977), p. 356.

31) Y. Nishiyama and H. Wise, *J. Catal.*, **32**, 50 (1974).

32) G. K. Hori and L. D. Schmidt, *J. Catal.*, **38**, 335 (1975).

33) R. G. Donnelly, M. Modell, and R. F. Baddour, *J. Catal.*, **53**, 239 (1978).

34) T. Okuhara and M. Misono, *Hyomen*, **18**, 357 (1980).

35) H. P. Bonzel and J. J. Burton, *Surf. Sci.*, **52**, 223 (1975).

36) According to our preliminary ^{18}O-tracer experiments, a considerable amount of $C^{16}O^{16}O$ was obtained by the reaction of $C^{16}O$ with $^{18}O_2$ on the Pt–V_2O_5/Al_2O_3 catalyst. This means that the reduced site, [Pt V], is considerably reoxidized by the bulk oxygen of V_2O_5 and that the V^{4+} in V_2O_5 thus produced is oxidized by $^{18}O_2$. The details of the results will be reported in a subsequent paper.

37) R. L. Palmer and J. N. Smith, Jr., *J. Chem. Phys.*, **60**, 1453 (1974).

38) A. W. Sklyarov, J. Voelter, and I. I. Tretjakov, *Z. Anorg. Allg. Chem.*, **396**, 129 (1973).

39) H. D. Cochran, R. G. Donnelly, M. Modell, and R. F. Baddour, *Colloid Interface Sci.*, **3**, 131 (1976).

40) N. W. Cant, P. C. Hicks, and B. S. Lennon, *J. Catal.*, **54**, 372 (1978).

41) A. Golchet and J. M. White, *J. Catal.*, **53**, 266 (1978).

42) P. Öser, *SAE Paper*, 790306 (1979).

43) W. M. Wang, *SAE Paper*, 800052 (1980).